Link sito dell'editore: https://www.elsevier.com/books-and-journals/elsevier

Link codice DOI: 10.1016/j.fuel.2017.04.117

Citazione bibliografica dell'articolo:

Ghanbari, M., Najafi, G., Ghobadian, B., Yusaf, T., Carlucci, A.P., Kiani Deh Kiani, M. "Performance and emission characteristics of a CI engine using nano particles additives in biodiesel-diesel blends and modeling with GP approach", pubblicato in Fuel, 2017, vol. 202, pagg. 699-716

Full Length Article

Performance and emission characteristics of a CI engine using nano particles additives in biodiesel-diesel blends and modeling with GP approach

M. Ghanbari[a]

G. Najafi[a, *]

g.najafi@modares.ac.ir

B. Ghobadian[a]

T. Yusaf[b]

A.P. Carlucci[c]

M. Kiani[d]

[a]Tarbiat Modares University, Tehran, Iran

[b]Faculty of Engineering and Surveying, USQ University, Toowoomba, Australia

[c]University of Salento, Lecce, Italy

[d]Shahid Chamran University of Ahwaz, Iran

*Corresponding author.

Abstract

The performance and the exhaust emissions of a diesel engine operating on nano-diesel-biodiesel blended fuels has been investigated. Multi wall carbon nano tubes (CNT) (40, 80 and 120 ppm) and nano silver particles (40, 80 and 120 ppm) were produced and added as additive to the biodiesel-diesel blended fuel. Six cylinders, four-stroke diesel engine was fuelled with these new blended fuels and operated at different engine speeds. Experimental test results indicated the fact that adding nano particles to diesel and biodiesel fuels, increased diesel engine performance variables including engine power and torque output up to 2% and brake specific fuel consumption (bsfc) was decreased 7.08% compared to the net diesel fuel. CO_2 emission increased maximum 17.03% and CO emission in a biodiesel-diesel fuel with nano-particles was lower significantly (25.17%) compared to pure diesel fuel. UHC emission with silver nano-diesel-biodiesel blended fuel decreased (28.56%) while with fuels that contains CNT nano particles increased maximum 14.21%. With adding nano particles to the blended fuels, NOx increased 25.32% compared to the net diesel fuel. This study also presents genetic programming (GP) based model to predict the performance and emission parameters of a CI engine in terms of nano-fuels and engine speed. Experimental studies were completed to obtain training and testing data. The optimum models were selected according to statistical criteria of root mean square error (RMSE) and coefficient of determination (R^2). It was observed that the GP model can predict engine performance and emission parameters with correlation coefficient (R^2) in the range of 0.93–1 and RMSE was found to be near zero. The simulation results demonstrated that GP model is a good tool to predict the CI engine performance and emission parameters.

Keywords: Nano additives; Diesel-biodiesel blends; Ultrasonic; Genetic programming

1 Introduction

The CI engines are widely utilized due to its reliable operation and economy. As the petroleum reserves are depleting at a faster rate, an urgent need for a renewable alternative fuel arise. Also the threat of global warming and the stringent government regulation made the engine manufacturers and the consumers to follow the emission norms to save the environment from pollution.

Among the many alternative fuels, biodiesel is considered as a most desirable fuel extender and fuel additive due to its high oxygen content and renewable in nature [1]. Among the various techniques available to reduce exhaust emissions, the utilize of fuel-borne catalyst is currently focused due to the advantage of increase in fuel efficiency while reducing greenhouse gas emissions. The influence of cerium oxide additive on ultrafine diesel particle emissions and kinetics of oxidation was studied by Jung et al. [2]. It has been

detected that addition of cerium to diesel cause significant reduction in number weighted size distributions and light-off temperature and the oxidation rate was increased significantly.

The structural and morphological characterization of a Ce-Zr mixed oxide supported Mn oxide as well as on its catalytic activity in the oxidation of particulate matter arising from diesel engines has been studied by Escribano et al. [3]. Mn-Ce-Zr catalyst shows high activity in the soot oxidation producing CO_2 and CO as a byproduct in the range 425–725 °K. Idriss investigated the complexity of the ethanol reactions on the surfaces of noble metals/cerium oxide catalysts [4]. The hazard and risk assessment with the use of nano-particle cerium oxide bases diesel fuel was studied by Barry Park et al. [5]. Effects of cerium oxide nano-particles addition in diesel and diesel-biodiesel-ethanol blends on performance and emission characteristics of a CI engine has been studied and results showed that the cerium oxide acts as an oxygen donating catalyst and provides oxygen for the oxidation of CO or absorbs oxygen for the reduction of NOx. The activation energy of cerium oxide acts to burn off carbon deposits within the engine cylinder at the wall temperature and prevents the deposition of non-polar compounds on the cylinder wall results reduction in HC emissions. The tests revealed that cerium oxide nano-particles can be used as additive in diesel and diesel-biodiesel-ethanol blend to improve complete combustion of the fuel and reduce the exhaust emissions significantly [1]. Carbon nano-tubes (CNTs) are as useful additives for increasing the octane number. Functionalized carbon nanotubes containing amide groups have a high reactivity and can react with many chemicals. These compounds can be solubilized in gasoline to increase the octane number. In a study, the amino-functionalized carbon nano-tubes were added to gasoline. Research octane number analysis showed that these additives increase octane number of the desired samples [6].

Experimental investigations to measure the performance and emission parameters of internal combustion engines are complex, time consuming and costly. To predict the parameters from the engines, one approach is to utilize numerical models [7]. The alternative to a mathematical model is the experiment-based approach. Genetic algorithm (GA), which is based on solutions of fixed length chromosomes, usually consisting of binary genes, organized into sequences, often termed schema is the most commonly used evolutionary-computation algorithm [8,9]. Evolutionary computation (EC) is drawing attentions for solving real engineering problems. This approach is to be robust in delivering global optimal solutions and coping with the restrictions encountered in traditional methods. EC harnesses the power of natural selection to turn computers into optimization tools [10–13]. This is very applicable to different problems in the manufacturing industry [11–17].

One of most important EC methods is genetic programming (GP). GP is a similar technique as genetic algorithm, an evolutionary computation method for imitating biological evolution of living organisms. Genetic Algorithms (GAs) and genetic programming (GP) have been found to offer advantages dealing with system modeling and optimization, especially for complex and nonlinear systems. GP has been applied to a wide range of problems in artificial intelligence, engineering and science, chemical and biological processes and mechanical issues [18–22]. Pires, et al. [23] used GP method to predict the next day hourly average tropospheric ozone (O_3) concentrations. The results showed very good agreement between predicted and measured data. Prediction of compressive and tensile strength of limestone was carried out via genetic programming as reported by Baykasoglu, et al., [24]. Another interesting genetic programming application was conducted by Cevik and Cabalar [25] for prediction of peak ground acceleration (PGA) using strong-ground-motion data. In this research, they demonstrated a high correlation between PGA and predictions. Multigene genetic programming is a recently developed approach for improving accuracy of GP that was developed by Hinchliffe, Willis, Hiden, Tham, McKay and Barton [26] and Hiden [27] and have been utilized in some recent research works [28,29]. Kiani et al. [30] studied the application of genetic programming to predict an SI engine brake power and torque using ethanol-gasoline fuel blends. At this study, the optimum models were selected according to statistical criteria of root mean square error (RMSE) and coefficient of determination (R^2). The values of RMSE and R^2 for brake power were found to be 0.388 and 0.998. It was observed that the GP model can predict engine torque with correlation coefficient in the range of 0.99–1 and RMSE was found to be 0.731. The simulation results demonstrated that GP model is a good tool to predict the engine brake power and torque under test [30]. Numerous studies have been under taken by using GA for optimization of engine characteristics [31–41]. Numerous studies have been undertaken by using genetic programming (GP) [42–46]. GP has been utilized to construct prediction model for diagnosing the engine valve faults. Kalogirou [47] reviewed ANN and GP for the modeling and control of engine combustion. A GP based mathematical model developed for the prediction of SI engine torque and brake specific fuel consumption in terms of spark advance, throttle position and engine speed [48,49].

The properties, combustion- and emission parameters of some common bio-fuels used in diesel engines as used under both steady-state and transient conditions, has been investigated [65,66].

In the present research study, the stable diesel biodiesel blends are prepared using vegetable waste oil methyl ester as additive and the emission reduction potential are investigated using nano silver and carbon nano tubes particles as fuel borne additive with neat diesel and diesel-biodiesel blends on the compression ignition engine. Parallel a multi-gene genetic programming (GP) algorithm based mathematical model for predicting an CI engine performance parameters and emission parameters in relation to input variables including engine speed, and nano-particles in diesel-biodiesel fuel blends.

The innovative characteristics of the present study compared to existing similar studies is utilize the new nano particles and additives with diesel-biodiesel blended fuels to investigate the performance and emission parameters of CI engine. This study also presents genetic programming (GP) based model to predict the performance and emission parameters of a CI engine in terms of nano-fuels and engine speed. Experimental studies were completed to obtain training and testing data.

2 Experimental work

2.1 Description of the experimental setup

In this study, the experiments were performed on a CI engine, 6 Cylinder, naturally aspirated, direct injection; fuel injection system of engine was solid and mechanical injection with distributer system. The shape of combustion chamber was Shallow depth chamber. Fuel injector type was single hole nozzle with hole diameter of 0.2 mm and spray cone angle obtained ranges from 5 to 20 degree, it requires high injection pressure in the range of 150–180 bar. The engine specification is given in Table 1. A 190 kW SCHENCK-WT190 eddy–current dynamometer was used in the experiments. Fuel consumption rate was measured in the range of 0.4–45 kg/h by using laminar type flow meter, Pierburg model. The measuring precision error for the calibration factors was ±0.1%, according to the DIN 1319 standard. The confidence level for this model was around 95%. Air consumption was measured using an AVL Flowsonix air flow meter. The measurement range was 0… ±1400 kg/h, with the error of <± 1%. The relative air–fuel ratio, the emission parameters and the exhaust gas temperature from an online and accurately calibrated exhaust gas analyser DIGAS4000 were recorded. The emission parameters from an online and accurately calibrated exhaust gas analyser DIGAS 4000 were recorded. AVL DIGAS analyzer is

used to measure the exhaust constituents such as CO, HC and NO_x. The sensitivity and the measurement accuracy of the instruments used for measuring the exhaust gas concentration have been listed in Table 2. The testing temperature was controlled, and temperature measurement accuracy was ±1 °C.

Table 1 Main characteristics of the test engine.

Engine Type	CI engine, 6 Cylinder
Combustion Order	1-5-3-6-2-4
Bore × Stroke(mm)	98.6 * 127
Comparison Ratio	17:1
Displacement Volume (Lit)	5.8
Max. Torque (N.m/rpm)	410/1300
Max. Power (kW/rpm)	82/2300

Table 2 The sensitivity and the measurement accuracy of the instruments used for measuring the exhaust gas concentration.

Exhaust gas	Measurements domain	Measurements accuracy	Measuring method
CO	0–15% vol.	0.06% vol.	Infrared meth.
CO_2	0–20% vol.	0.5% vol.	Infrared meth.
HC	0–2000 ppm	12 ppm	Infrared meth.
NO_x	0–5000 ppm	32–120 ppm	Electronic meth.

Separate fuel tanks were fitted to the diesel engine and these contained diesel and the biodiesel–diesel blends. Fig. 1 shows the schematic diagram of the experimental setup. Also the use of carbon nano tubes (CNT) and silver nano particles in neat diesel and diesel-biodiesel blend has the tendency to settle down at the fuel tank. B20 (B20 or BD: 20%vol. Biodiesel and 80%vol. diesel blend), silver nano particle with the size of 50 nm and CNT nano particle with the diameter of 5 nm are used in the test. After series of experiments, it is found that the blends subjected to high speed blending followed by ultrasonic bath stabilization improves the stability. Vegetable methyl ester (Biodiesel) prepared from the waste cooking oil (WCO) through transestrification process (Fig. 2), and then blended with diesel fuel. The performance tests for the diesel-biodiesel blends and neat diesel with nano silver and CNT nano particles as fuel-borne catalyst additive are carried out on a computerized diesel engine. A computerized data acquisition system is used to collect, store and analyze the data. All tests were carried out at full load (WTO) condition. An important criterion of the full load performance is the maximum torque value as compared to that in the engine specification, so due to investigate the variation of performance and emission parameters at critical condition, the full load was selected. The load applied on the engine is measured by the load cell connected to the eddy current dynamometer. All the experiments are conducted and the results are recorded under steady state conditions.

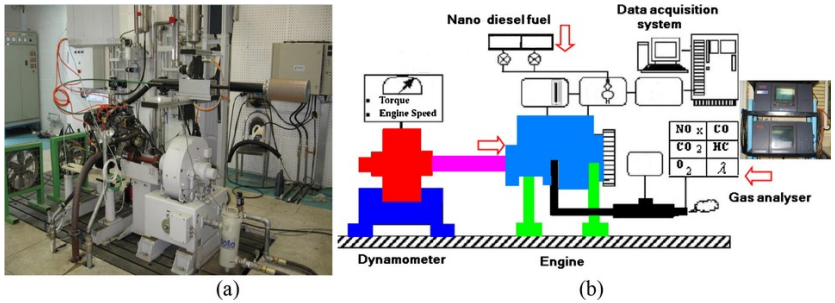

Fig. 1 Engine test set-up and test instruments (a) real and (b) schematic.

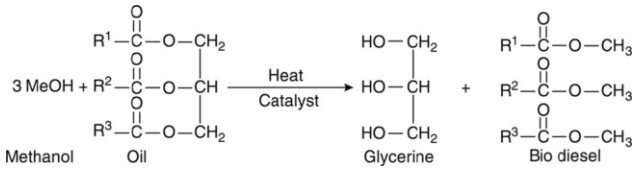

Fig. 2 Transestrification reaction of waste cooking oil with methanol in the presence of catalyst [50,51].

In transestrification process, the KOH (grade 99%) and methanol (grade 99.9%) were prepared from Merck Chemical Industries, Germany, and was utilized without further purification. Also, the required standards were needed to be considered in GC device (i.e. the methyl ester of fatty acids C18:2, C18:1, C18:3, C16:1 and C16:0) and n-heptanes were provided by Sigma-Aldrich Company. A Gas Chromatography (GC) unit of Perkin Elmer clarus on BS-EN standard were used for biodiesel yield and percentage of methyl ester content of the produced biodiesel. The purified methylated using Metcalf method, and the prepared sample was injected into GC device in order to determine fatty acids profile and molecular weight of the used oil (Fig. 3). The physical and chemical properties of WCO and the chromatogram of the WCO for this investigation are shown in Table 3 and Fig. 3c, respectively. The produced Biodiesel properties in comparison with ASTM D6751 standard has been described in Table 4.

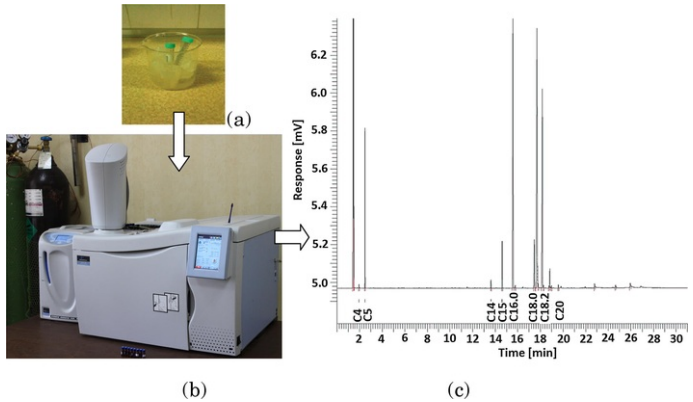

Fig. 3 (a) samples, (b) gas chromatography (GC) analyzer and (c) the yields of fish oil compounds according to the carbon numbers in the chain by GC.

Table 3 Chemical and physical properties of the used WCO.

Properties	Units	Measured Property
Density	g/cm^3	0.905
Kinematic viscosity	mPa·s	25.580
Acid value	Mg KOH/g oil	0.98
Iodine value	g I_2/100 g oil	112.5
Water content	mg/g	0.15
Palmitic acid (C16:0)	wt.%	10.71
Stearic acid (C18:0)	wt.%	2.45
Oleic acid (C18:1)*	wt.%	22.90
Linoleic acid (C18:2)*	wt.%	55.01
Linoleic acid (C18:3)*	wt.%	2.67
Other fatty acids	wt.%	6.26

Mean molecular weight of WCO	g/mol	876.60

* Carbon atoms number: double bond number.

Table 4 The Produced Biodiesel Properties in comparison with ASTM D6751 standard.

Property	Test Method	Limits	Units	Measured Property
Water and Sediment	ASTMD2709	0.05max	%volume	0.045
Kinematic Viscosity @ 40 °C	ASTMD445	1.9–6.0	mm2/s	3.5
Sulfated Ash	ASTMD874	0.02max	%mass	0.01
Sulfur S 15 Grade	ASTMD5453	0.0015max	%mass	0.001
Sulfur S 500 Grade	ASTMD5453	0.05max	%mass	–
Copper Strip Corrosion	ASTMD130	No3max		No 2
Methanol Content	EN14110	0.20max	%volume	0.15
Flash Point, Closed Cup	D93	130 min	◦C	170
Cetane Number	ASTMD613	–		45
Carbon Residue	ASTMD4530	0.05max	%mass	0.02
Acid Number	ASTMD664	0.50max	mgKOH/g	0.34
Free Glycerin	ASTMD6584	0.02	%mass	0.01
Total Glycerin	ASTMD6584	0.24	%mass	0.01
Phosphorus	ASTMD4951	10max	ppm	–
Vacuum Distillation End Point	ASTMD1160	360°Cmax	°C	–
Oxidative Stability	EN14112	3 min	hours	2.2
Cold Soak Filtration	Annex toD6751	360max	seconds	240

An ultrasonic processor (UP400S, Hielscher, USA) was used to perform the transestrification reaction and even mixing biodiesel and nano-particles before the engine tests. The equipment consisted of the processor, the sonotrode, and the PC control (UPC400T). The processor operated at 400 W and 24 kHz frequency. The amplitude and the pulse for the reaction were adjustable from 20 to 100%. The titanium sonotrode (H22D) with a diameter of 22 mm and a length of 100 mm was used to transmit the ultrasound into the liquid. According to the results of similar studies for optimal reaction temperature, reaction temperature as an effective factor in reaction efficiency, was kept constant at 45 °C by a circulator apparatus test set. The schematic diagram of the experimental set-up used in this study is shown in Fig. 4.

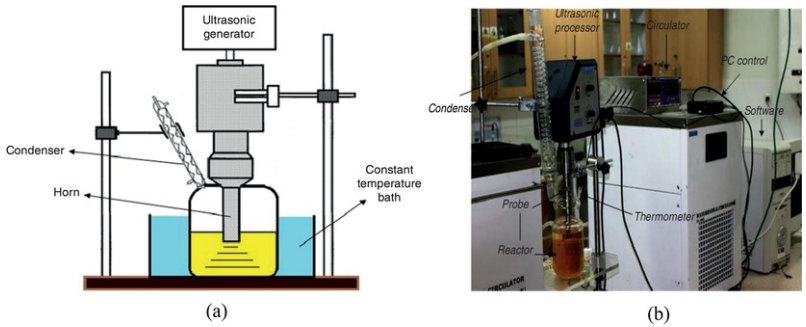

Fig. 4 The set-up for ultrasonic assisted nano-biodiesel-diesel production process:(a) schematic and (b) real.

Considering the accomplished researches about nano fuels and diesel fuel nano additives, two silver nano-particles (Ag) and carbon nano tubes (CNT) were applied as nano additives to these fuels. Furthermore based on researches conducted about the effect of concentrations of used nano-particles in reduction of exhaust emissions, in this study three concentrations (40, 80 and 120 ppm) were applied. In order to ensure the validity of nano-particles utilized in this research, SEM and TEM pictures were taken (Fig. 5).

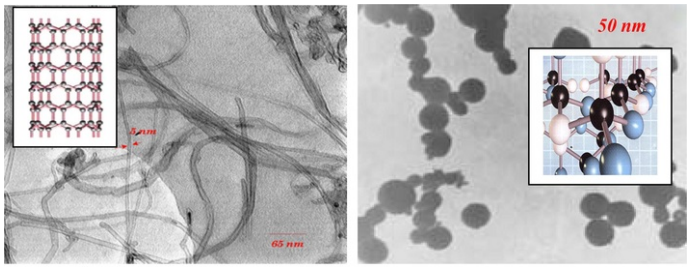

(a) (b)

Fig. 5 TEM image of (a) the CNT nano particles, (b) silver nano particles.

Nano silver and Multi-walled carbon nano-tubes with 90–95% purity prepared by CVD method over Co-Mo/MgO catalyst [52,53]. The average diameter of the nano tubes varies from 5 to 20 nm and their length from 5 to 15 μm. Specification of fuels and applied nano-additives with different concentrations are indicated in Table 5. Fig. 6 indicates a general schematic picture of the whole experiment and the equipments were being used.

Table 5 Fuels, Nano-additives and their concentrations.

Fuel	Nano-particles	Nano Concentration (PPM)
Diesel	Nano-silver (Ag)	40
		80
		120
Biodiesel (B20=20% biodiesel+80% diesel fuel)	Carbon Nano-Tubes (CNT)	40
		80
		120

Carbon nanotubes has been produced and available for both research and industrial purposing. The production cost of the nanotubes additives in diesel and biodiesel blends in diesel engine was $3 per gram.

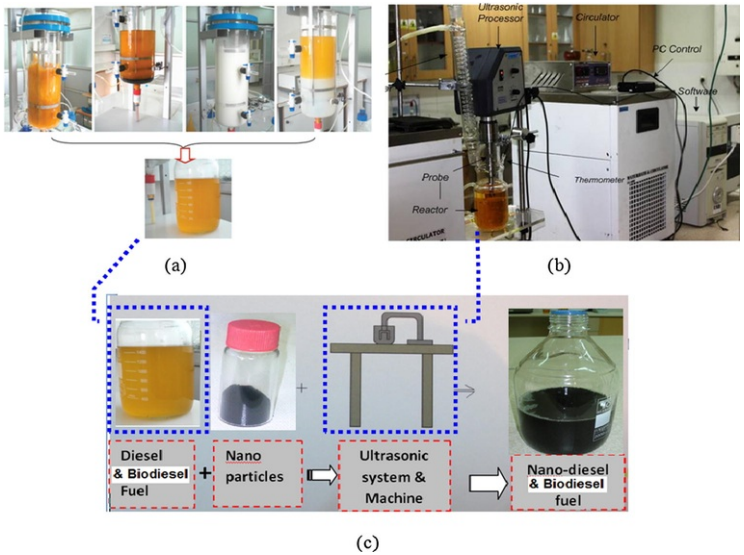

Fig. 6 The Set up for ultrasonic-assisted nano-diesel production process (a) transestrification reaction, (b) ultrasonic set-up and (c) nano-diesel-biodiesel blend.

2.2 Testing procedure

The performance and emission from the CI engine running on biodiesel (derived from vegetable cooking oil) and blended with diesel fuel were evaluated and compared with diesel fuel. A Hielscher ultrasonic processor (UP400S) was utilized for mixing biodiesel, diesel and nano-particles before the engine tests. In the first phase, experiments were performed with the biodiesel (B20) in five engine speeds 800,850, 900, 950 and 1000 rpm. Next, silver and CNT nano-particles with concentrations of 40, 80 and 120 ppm were added to biodiesel.

Above 20% biodiesel, some parts of engine should be modified; therefore, only experimental results obtained up to this percentage of biodiesel will be presented. The fuel blends were prepared just before starting the experiment to ensure that the fuel mixture was homogenous. A series of experiments were carried out using diesel, and biodiesel blends. All the blends were tested under varying engine speed conditions. The engine was started using diesel fuel and it was operated until it reached the steady state condition. The engine speed, fuel consumption, and load were measured, while the brake power, brake specific fuel consumption (bsfc), were computed. After the engine reached the stabilized working condition, emission parameters such as CO, CO_2, HC, NO_x from an online and accurately calibrated exhaust gas analyser were recorded. All experiments have been carried out at full load conditions.

3 Experimental results

3.1 Engine performance

3.1.1 Brake power and torque output

Fig. 7 shows the effect of various fuels on engine brake power. When the nano content in the diesel fuel and diesel-biodiesel blended fuel is increased, the engine brake power slightly increased for all engine speeds. The gain of the engine power can be attributed to the increase of the indicated mean effective pressure for higher nano content blends [54]. The heat of evaporation of nano-diesel is higher than that diesel fuel, this provides fuel–air charge cooling and increases the density of the charge, and thus higher power output is obtained [55]. With the increase in concentration of nano silver and carbon nano tubes, the density of the mixture and the engine volumetric efficiency increases and this causes the increase of power [56]. The addition of nano particles with neat diesel and diesel-biodiesel blends accelerates early initiation of combustion and the ignition delay decreases. The addition of biodiesel increases the ignition delay, hence more fuel is accumulated in the premixed combustion phase is the cause for faster combustion which results in higher peak pressure. Higher peak pressure causes to have higher brake power [1]. The brake power of CNT120-diesel-biodiesel is higher among all the fuel blends. The brake power of the nano-diesel blends is lower than nano-diesel-biodiesel blends. A small improvement in brake power is observed with the addition of nano particles with diesel and diesel-biodiesel blends. The highest brake power is observed as 2.03% for CNT120-D80-B20 blend whereas it is 1.84% for CNT120-D100 compared to the neat diesel fuel. Experimental results proved that the increase of nano particles content and biodiesel increases the torque of the engine. Added biodiesel produces lean mixtures that increase the relative air–fuel ratio to a higher value and makes the burning more efficient [57]. The improved antiknock behaviour (due to the addition of biodiesel and nano particles) allowed a more advanced timing that results in higher combustion pressure and thus higher torque [58]. A small improvement in brake torque is observed with the addition of nano particles with diesel and diesel-biodiesel blends. The highest brake torque is observed as 2% for CNT120-BD (Diesel 80%-Biodiesel 20% vol.) blend whereas it is 1.8% for CNT120-D100 compared to the neat diesel

fuel.

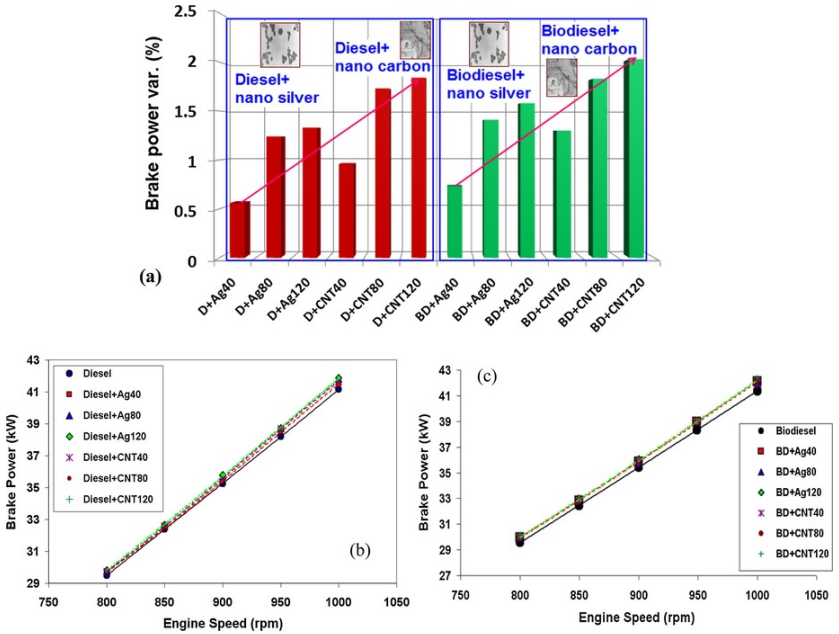

Fig. 7 (a) Brake power with nano-diesel-biodiesel blends compared to neat diesel fuel (1000 rpm), (b) brake power at different nano-diesel fuel blends and engine speeds and (c) brake power at different nano-biodiesel fuel blends and engine speeds.

3.1.2 Brake specific fuel consumption

The specific fuel consumption is lower for the nano-diesel and nano-diesel-biodiesel blends than neat diesel fuel at all the engine speed. This is due to higher calorific value of the diesel-biodiesel blend than neat diesel; less quantity of fuel is consumed to maintain the engine speed constant. As shown in Fig. 8, the bsfc decreases as the nano concentration increases. This phenomenon is due to the result of nano silver and CNT nano addition which promotes combustion [1]. The lowest bsfc observed as 202.96 g/kW.hr for the BD-CNT 120 blend whereas it is 222.18 g/kW.hr for neat diesel. The variation of bsfc with nano-diesel-biodiesel fuels is shown in Fig. 8. Improvement in bsfc is observed with the addition of nano particles with diesel and diesel-biodiesel blends. The highest decrease for bsfc is observed as 7.08% for CNT120-D80-B20 blend whereas it is 5.7% for CNT120-D100 compared to the neat diesel fuel.

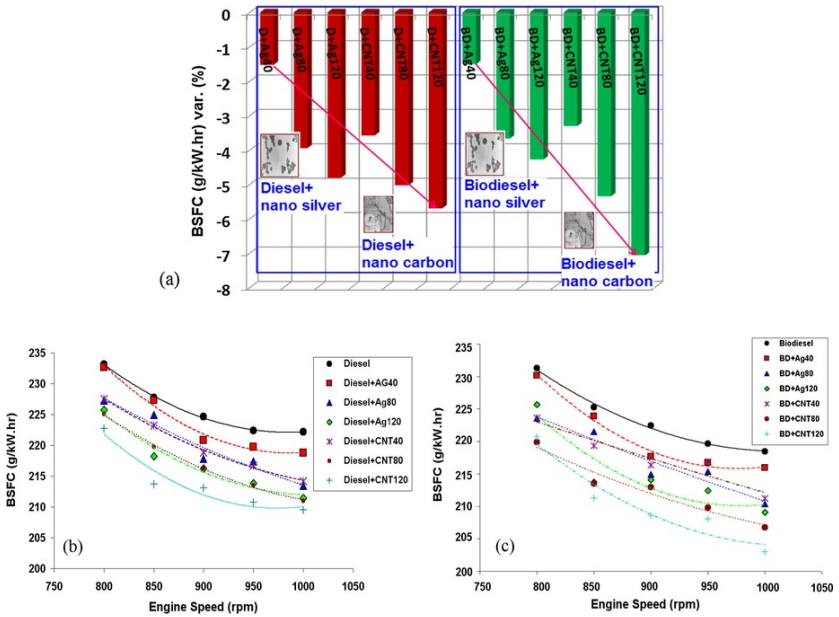

Fig. 8 (a) bsfc with nano-diesel-biodiesel blends compared to neat diesel fuel (1000 rpm), (b) bsfc at different nano-diesel fuel blends and engine speeds and (c) bsfc at different nano-biodiesel fuel blends and engine speeds.

3.2 Engine emissions

3.2.1 CO emission

Fig. 9 shows the concentrations of CO emission for different engine speeds and different fuel blends. The carbon monoxide emission decreases with the use of diesel-biodiesel-nano blends than neat diesel. It can be seen from this figure that when nano concentration increases, the CO concentration decreases which means the combustion is tuned to be completed. The addition of nano silver and carbon nano tubes particles further decreases the CO emission when comparing with neat diesel. The variation of CO emission with nano-diesel-biodiesel fuels is shown in Fig. 9. The CO of CNT120-diesel-biodiesel is lowest among all the fuel blends. The lowest CO emission is observed as 25.17% for CNT120-D80-B20 blend whereas it is 22.48% for CNT120-D100 compared to the neat diesel fuel.

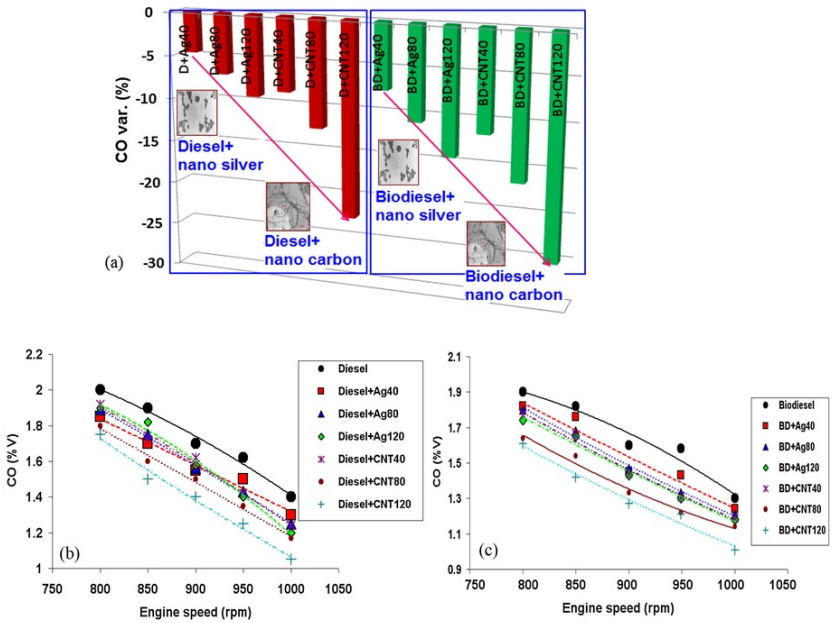

Fig. 9 (a) Variation of CO with nano-diesel-biodiesel blends compared to neat diesel fuel (1000 rpm), (b) CO at different nano-diesel fuel blends and engine speeds and (c) CO at different nano-biodiesel fuel blends and engine speeds.

3.2.2 CO_2 emission

Fig. 10 shows the relationship between the CO_2 concentrations and engine speeds for different blends percentage. Experimental results indicate that CO_2 concentration increases as the biodiesel and nano particles concentration increases. CO_2 emission depends on relative air–fuel ratio and CO emission concentration [55,60]. As a result of the lean burning associated with increasing nano particles, the CO_2 emission increased because of the improved combustion [56–60,49,61,21,62–68]. Variation of CO_2 with nano-diesel-biodiesel blends compared to neat diesel fuel has been indicated in Fig. 10.

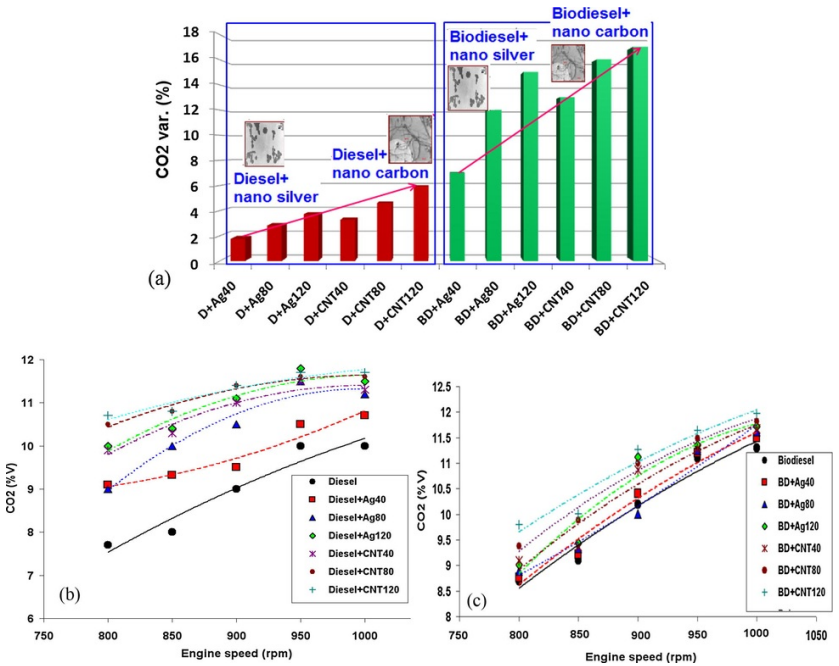

Fig. 10 (a) Variation of CO_2 with nano-diesel-biodiesel blends compared to neat diesel fuel (1000 rpm), (b) CO_2 at different nano-diesel fuel blends and engine speeds and (c) CO_2 at different nano-biodiesel fuel blends and engine speeds.

3.2.3 HC emission

HC emissions for different speeds and blended fuels are illustrated in Fig. 11. This result indicates that adding of nano particles and blending of biodiesel with diesel fuel can significantly reduce HC emissions. The concentration of HC emission decreases with the increase of the relative air–fuel ratio, the reason for the decrease of HC concentration is similar to that of CO concentration described above [57–60]. The addition of nano silver particles decreases the HC emission while addition of carbon nano tubes increases the HC emission when comparing with neat diesel fuel. The use of oxygenated additives promotes complete combustion is the cause for the hydrocarbon emission reduction, but in the case of CNT particles due to have carbon in their structure, HC emission increases [1]. The variation of HC with nano-diesel-biodiesel fuels is shown in Fig. 11. The highest decrease for HC is observed as 28.56% for Ag120-BD blend whereas it is increased maximum 14.21% for CNT120-BD compared to the neat diesel fuel.

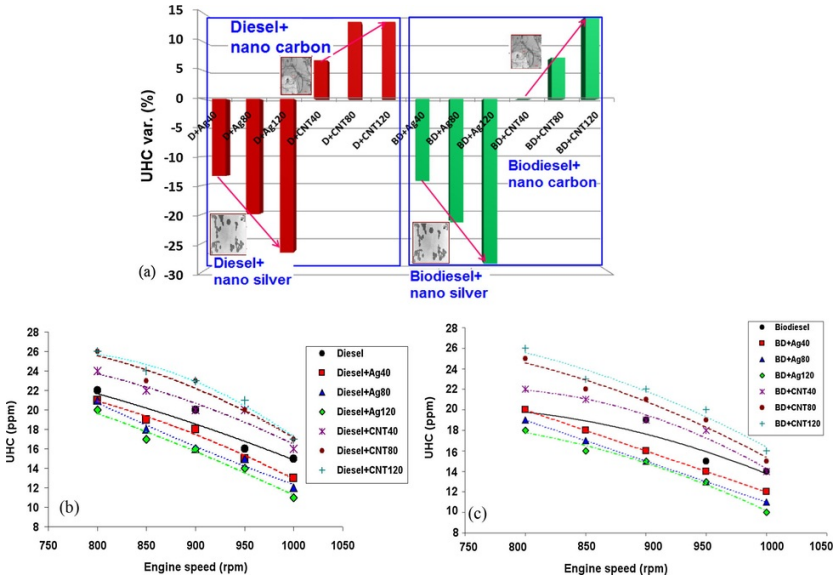

Fig. 11 (a) Variation of UHC with nano-diesel-biodiesel blends compared to neat diesel fuel (1000 rpm), (b) UHC at different nano-diesel fuel blends and engine speeds and (c) UHC at different nano-biodiesel fuel blends and engine speeds.

3.2.4 No_x emission

Considering the NO_x emission, Fig. 12 shows that the NO_x concentration is higher when nano particles concentration increases. It shows that as the concentration of nano particles in the blends increased, NO_x emission was increased. When the combustion process is closer to stoichiometric, flame temperature increases, therefore, the NO_x emission is increased, particularly by the increase of thermal NO [68–84]. The NO_x emission is lower for the neat diesel when comparing to all the fuel blends. The effect of oxygenated additives enhances combustion and the longer ignition delay due to biodiesel and nano particles addition results in faster premixed combustion is the cause for higher combustion temperature and the subsequent higher NO_x emission. Variation of NO_x with nano-diesel-biodiesel blends compared to neat diesel fuel has been indicated in Fig. 12.

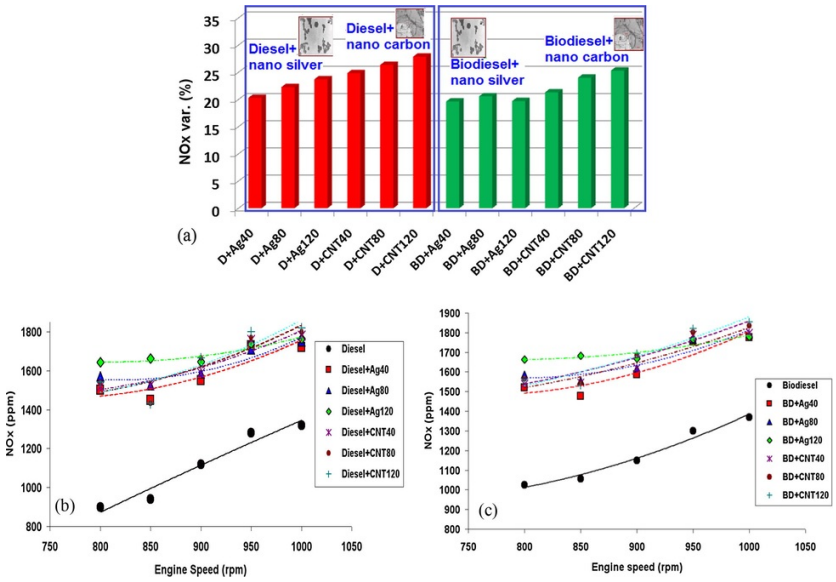

Fig. 12 (a) Variation of NO_x with nano-diesel-biodiesel blends compared to neat diesel fuel (1000 rpm), (b) NO_x at different nano-diesel fuel blends and engine speeds and (c) NO_x at different nano-biodiesel fuel blends and engine speeds.

It should be mentioned that operating discrepancies such as injector clogging on CI engine operation mainly during operation with biodiesel and additives has not been observed.

4 GP model development

4.1 Overview of genetic programming

Genetic programming (GP) is a sub-branch of evolutionary algorithms (EAs) emulating the natural evolution of species. Genetic programming (GP) technique is an extension to Genetic Algorithm (GA). The main difference between GA and GP resides in the nature of the individuals: in GAs the individuals are symbolic strings of fixed length (chromosomes); in GP the individuals are nonlinear entities of different sizes and shapes (parse trees) [49].

Koza [61] was one of the scientists who first suggested the use of GP to find a symbolic regression tree matching to the mathematical formula which can best fit the data according to a fitness criterion. Fitting such a model was performed in an optimization frame work in which the error of the created symbolic trees versus sample data is minimized via regression. Thus, it is intrinsically suitable for modeling of complex industrial problems. In order to emulate the evolutionary process in the design of GP, certain components should be defined. These include n-ary arithmetic functions, problem decision variables and evolutionary operators such as reproduction, crossover, and mutation to symbolic expressions. The symbolic expressions, called individuals or solutions, are generated to create the initial population. A population in evolutionary algorithms is a set of a defined number of solutions at an iteration of the algorithm. The initial expressions are produced with tree-based encoding. For instance, the mathematical expression ($(b * x_1 + \sin(x_3)) * \tanh(a * x_2)$) can be indicated by diagram as shown in Fig. 13. These expressions are constituted of elements from two distinctive parameter groups: (i) a functional set and (ii) a terminal set. The functional set is generally arithmetic function, e.g. f = {*, +, −, sin, cos, log, power …}. The arguments for these functions are supplied from the terminal set that includes the decision variables and constants. For instance, in Fig. 13 the function set (F) is composed of F = {*, +, sin, tanh} and the terminal set (T) is composed of T = {x_1, x_2, x_3, a, b}. The initial solutions are restricted in terms of tree depth or length of expression to fill the first population in the algorithm with the potential building blocks of individuals to be created at the next step of the algorithm. A basic flowchart of the genetic programming model has been presented in Fig. 14.

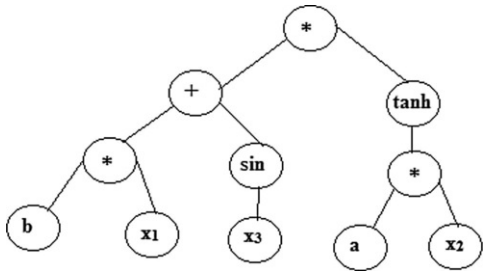

Fig. 13 Example of tree representation of mathematical expressions used in GP.

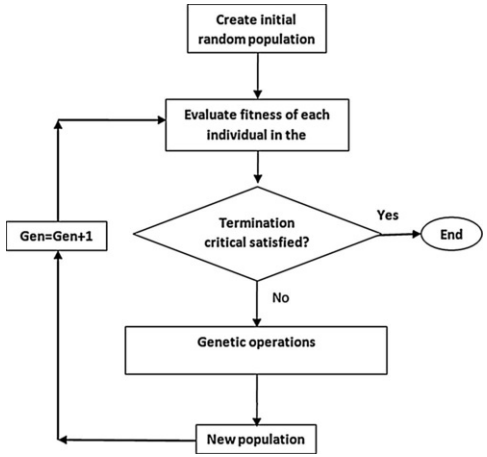

Fig. 14 Flow chart of the genetic programming paradigm.

At each generation a new population is created through selecting individuals based on their fitness and using the genetic operators (reproduction, crossover, and mutation). In reproduction operation, part of population (the fittest individuals) is preserved so that new generation is the result of genetic operations on the individuals of the actual population. In crossover operation two individuals (parents) are selected, their tree structures are broken at a randomly selected crossover point, and the produced sub-trees are recombined to form two new individuals (offspring) [21]. Fig. 15 demonstrates the crossover operation. Mutation operation includes selecting an individual, randomly choosing a branch and deleting and replacing it with a new random branch (Fig. 16). The existing population will then be substituted with the new population. The procedure is iterated until a termination criterion (achievement of the maximum number of generations or a determined error defined) is satisfied.

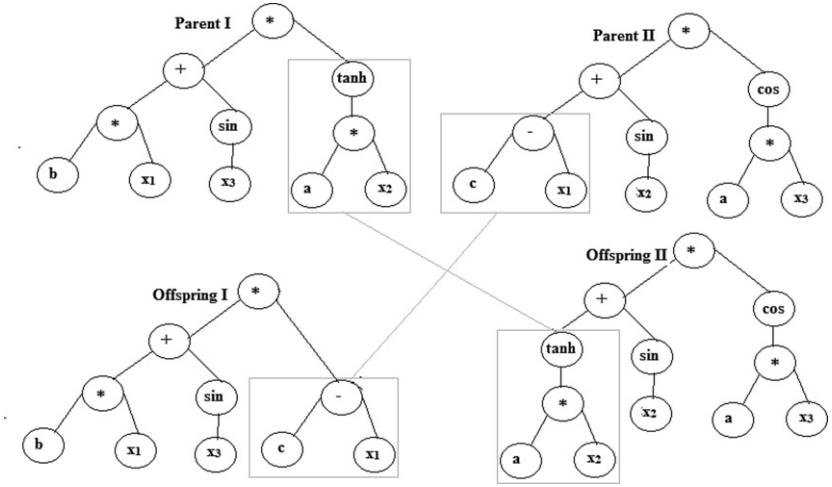

Fig. 15 Crossover operation between two parents.

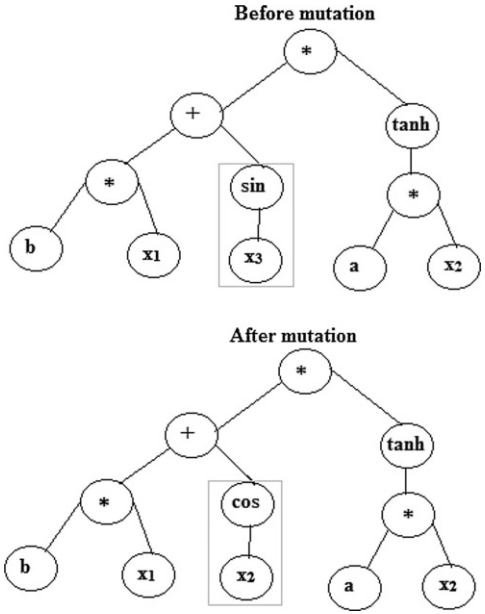

Fig. 16 Mutation operation in individual.

In reproduction operation, part of population (the fittest individuals) is preserved so that new generation is the result of genetic operations on the individuals of the actual population. In crossover operation two individuals (parents) are selected, their tree structures

are broken at a randomly selected crossover point, and the produced sub-trees are recombined to form two individuals (offspring) [62]. The existing population will then be substituted with the new population. The procedure is iterated until a termination criterion (achievement of the maximum number of generations or a determined error defined) is satisfied. A newly developed method for improving the precision of GP is "multi-gene genetic programming". The main difference between the traditional and the multi-gene GP is the number of trees which can be used. In the traditional GP, a single tree represents the model however, in the multi-gene GP several trees may express the model. All of these genes possess specific optimal weights and sum of weighted genes plus a bias term would form the final formula as the best resulted numerical model. Multi-gene GP can be shown as the follow:

$$Y = a_0 + a_1 \times gene_1 + a_2 \times gene_2 + \ldots + a_n \times gene_n \quad (1)$$

In which, a_0 is the bias term and a_i is weight of the i_{th} gene. Indeed, multi-gene GP is a linear combination of nonlinear terms, and this feature allows identifying the model of engineering problems in a highly precise manner.

4.2 Modeling with GP

The GP was used in this study to perform a multi-gene genetic programming for precise prediction of diesel engine performance (power, torque, BSFC) and emission (CO, CO_2, UHC and NO_x) parameters. The genetic programming and Symbolic Regression is a new code that has been written on the basis of multi-gene GP for utilize with MATLAB [63]. The GP has the possibility of setting some limitations to avoid bloating. Bloating is defined as the unnecessary growth of the model without any significant improvement in the fitness. In order to avoid bloating, some restrictions were imposed on initial parameters such as maximum number of genes, maximum depth of genes and trees, and maximum number of nodes per tree. In addition, lexicographic tournament selection that is an efficient method for restraining the model bloating was utilized in GP. It is noteworthy that the present investigation has considered root mean square error (RMSE) as the fitness function of the analysis. The RMSE is defined as:

$$RMSE = \sqrt{\frac{1}{n}\sum_{i=1}^{n}(t_i - o_i)^2} \quad (2)$$

where t is the experimental value, o is the predicted value and n is the total number of data. Table 6 indicates the range of the initial parameters used in the GP runs. Other initial parameters were adjusted to their default values in GPTIPS, according to Searson [64].

Table 6 Multi-gene GP ranges of initially parameters.

Parameter	Range
Number of generations	100–300
Population size	100–400
Function set	{+,−,×,√,÷, sin, cos, exp, log, tanh}
Max. number of genes	3–5
Max. depth of tree	4–8
Probability of crossover	0.70–0.95
Probability of mutation	0.04–0.2
Probability of reproduction	0.01–0.1

Three statistical evaluation criteria were applied to assess the model performance:

(i) The root mean square error (RMSE) (Eq. (2)), (ii) The coefficient of determination (R^2) defined in Eq. (3) and (iii) Variation explained (VE) has been described at Eq. (4):

$$R^2 = \left(1 - \frac{\sum_{i=1}^{n}(t_i - o_i)^2}{\sum_{i=1}^{n}(t_i - \bar{t}_i)^2}\right) \quad (3)$$

$$VE = 100 \times R^2 \quad (4)$$

For developing the GP model, the data (560 test in total), taken from the experimental study were used as training and testing sets for the GP architecture. Data was divided into two subsets including the training and testing with a ratio of 0.75 and 0.25, respectively.

4.2.1 Brake power

The following equation was selected as the best model for brake power.

$$BP = 0.9887x_1 + 0.07344x_3 + 0.03672square(\sin(x_1)) + 0.03744\sin(x_2x_3)(x_3 - 1.0) - 0.03744\sin(x_2x_3)(\sin(x_1) - \tanh(x_3)) - 0.02236 \quad (5)$$

where BP is the engine brake power (kW), and x1, x2 and x3 are the engine speed (rpm), Ag (ppm) and CNT (ppm) nano particle concentration, respectively. Accuracy of the equation is studied by plotting the measured values versus predicted by GP values for training and testing sets (Fig. 17). The values of R^2 and RMSE are 0.9995 and 0.0901 respectively for testing set (Fig. 17a) and 0.9998 & 0.0458 respectively for training set (Fig. 17b). There is a good correlation between the predictions from multi-gene GP and the measured data. A comparison of the error during testing and training by using GP and experimental results has been illustrated in Fig. 17c & d. It was proved that the multi-gene GP model can predict engine brake power with a high variation explained (99.95% for testing and 99.99% for training) and very low root mean square (RMS) error (0.09 for testing and 0.04 for training).

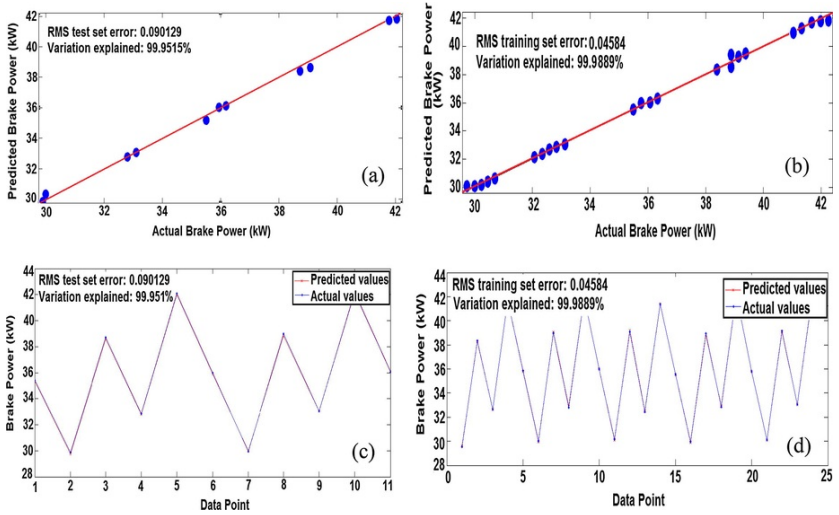

Fig. 17 Measured versus predicted values of brake power (a) testing set data, (b) training data set. Experimental results and the GP model prediction of brake power for (c) testing set data, (d) training data.

4.2.2 Torque

The following equation was selected as the best model for engine torque:

$$T = 0.9936x_1 + 0.8786\tanh(\exp(x_3)) + 0.23\sin(x_2) + 0.01404x_1(x_2 - 2x_1 + x_3) - 0.5181 \quad (6)$$

where T is the engine torque (Nm). Accuracy of the equation is studied by plotting the measured values versus predicted by GP values for training and testing sets (Fig. 18). The values of R^2 and RMSE are 0.9965 and 0.88868 respectively for testing set (Fig. 18a) and 0.9993 & 0.38851 respectively for training set (Fig. 18b). There is a good correlation between the predictions from multi-gene GP and the measured data. A comparison of the error during testing and training by using GP and experimental results has been illustrated in Fig. 18c & d. It was proved that the multi-gene GP model can predict engine torque with a high variation explained (99.95% for testing and 99.93% for training) and very low root mean square (RMS) error (0.88 for testing and 0.38 for training).

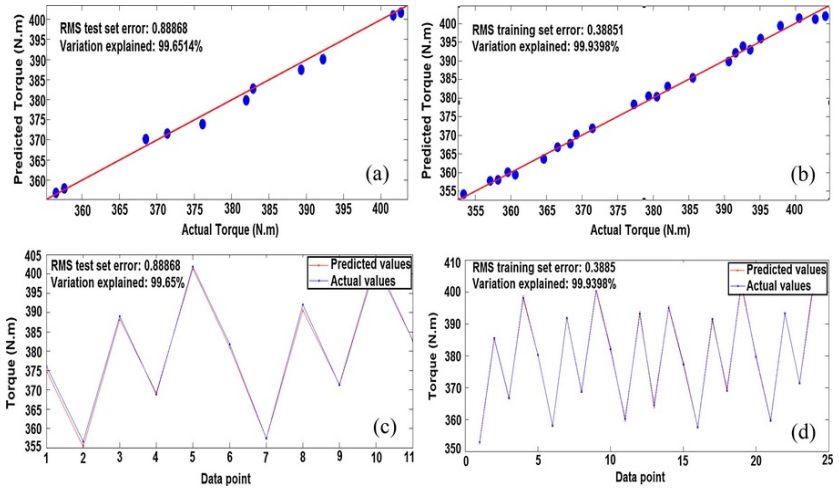

Fig. 18 Measured versus predicted values of torque (a) testing set data, (b) training data set. Experimental results and the GP model prediction of torque for (c) testing set data, (d) training data.

4.2.3 BSFC

The following equation was selected as the best model for brake specific fuel consumption:

$$BSFC = 1.494\sin(\sin(x_1 + x_3)) - 0.5299x_2 - 0.5299x_3 - 1.494x_1 - 1.494\tanh(\exp(x_3)) \\ -1.133\sin(x_1 + x_3) + 1.133\sin(\sin(\sin(x_1))) - 0.5299\cos(x_1) + 1.286 \quad (7)$$

where BSFC is the brake specific fuel consumption (g/kW.h). Accuracy of the equation is studied by plotting the measured values versus predicted by GP values for training and testing sets (Fig. 19). The values of R^2 and RMSE are 0.9477 and 1.5521 respectively for testing set (Fig. 19a) and 0.9678 & 1.15 respectively for training set (Fig. 19b). There is a good correlation between the predictions from multi-gene GP and the measured data. A comparison of the error during testing and training by using GP and experimental results has been illustrated in Fig. 19c & d. It was proved that the multi-gene GP model can predict BSFC with a high variation explained (94.77% for testing and 96.78% for training) and very low root mean square (RMS) error (1.55 for testing and 1.15 for training).

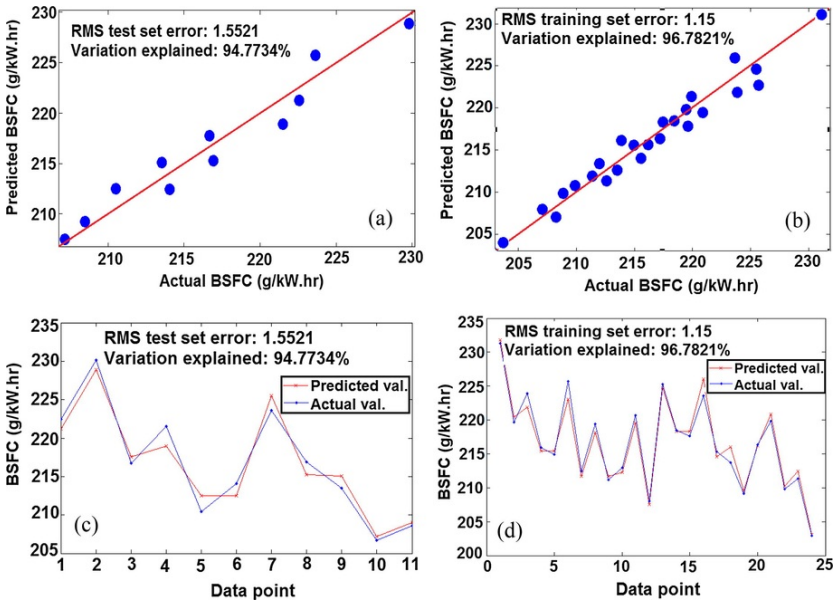

Fig. 19 Measured versus predicted values of brake specific fuel consumption (a) testing set data, (b) training data set. Experimental results and the GP model prediction of bsfc for (c) testing set data, (d) training data.

4.2.4 CO

The following equation was selected as the best model for CO emission:

$$CO = 0.3337x_3 + 2.276\sin(\tanh(x_2 - \exp(\sin(x_2)))) + 0.3337psqroot(p\log(x_3) - x_1) + 5.612\sin(\tanh(\exp(\tanh(\sin 9x_1)))) - 0.3337\sin(x_2 - x_3)p\log(\tanh(x_1)) - 2.305 \quad (8)$$

where CO is the CO emission (%Vol.). Accuracy of the equation is studied by plotting the measured values versus predicted by GP values for training and testing sets (Fig. 20). The values of R^2 and RMSE are 0.9337 and 0.2678 respectively for testing set (Fig. 20a) and 0.9922 & 0.0934 respectively for training set (Fig. 20b). There is a good correlation between the predictions from multi-gene GP and the measured data. A comparison of the error during testing and training by using GP and experimental results has been illustrated in Fig. 20c & d. It was proved that the multi-gene GP model can predict CO with a high variation explained (93.37% for testing and 99.28% for training) and very low root mean square (RMS) error (0.2678 for testing and 0.0934 for training).

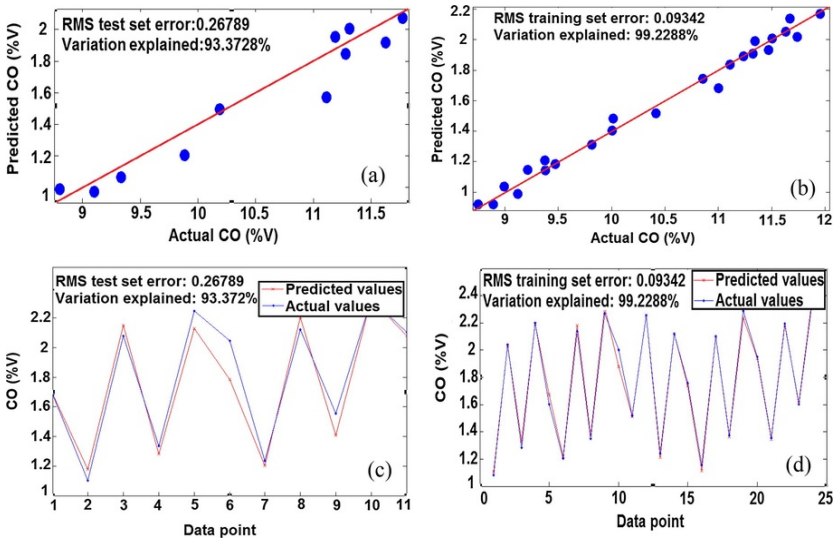

Fig. 20 Measured versus predicted values of CO emission (a) testing set data, (b) training data set. Experimental results and the GP model prediction of CO for (c) testing set data, (d) training data.

4.2.5 CO_2

The following equation was selected as the best model for CO_2 emission:

$$CO_2 = 0.2033x_2 + 0.2033x_3 + 0.2033\tanh(x_1 - x_2) + 0.2033\tanh(x_3 + \tanh(x_1)) - 0.3871psqroot(\tanh(\tanh(x_3)) - x_3 - \tanh(x_1)) + 1.373\tanh(\tanh(x_1)) + 0.3083 \quad (9)$$

where CO_2 is the CO_2 emission (%Vol.). Accuracy of the equation is studied by plotting the measured values versus predicted by GP values for training and testing sets (Fig. 21). The values of R^2 and RMSE are 0.9486 and 0.2358 respectively for testing set (Fig. 21a) and 0.9922 & 0.0936 respectively for training set (Fig. 21b). There is a good correlation between the predictions from multi-gene GP and the measured data. A comparison of the error during testing and training by using GP and experimental results has been illustrated in Fig. 21c & d. It was proved that the multi-gene GP model can predict CO_2 with a high variation explained (94.86% for testing and 99.22% for training) and very low root mean square (RMS) error (0.2358 for testing and 0.0936 for training).

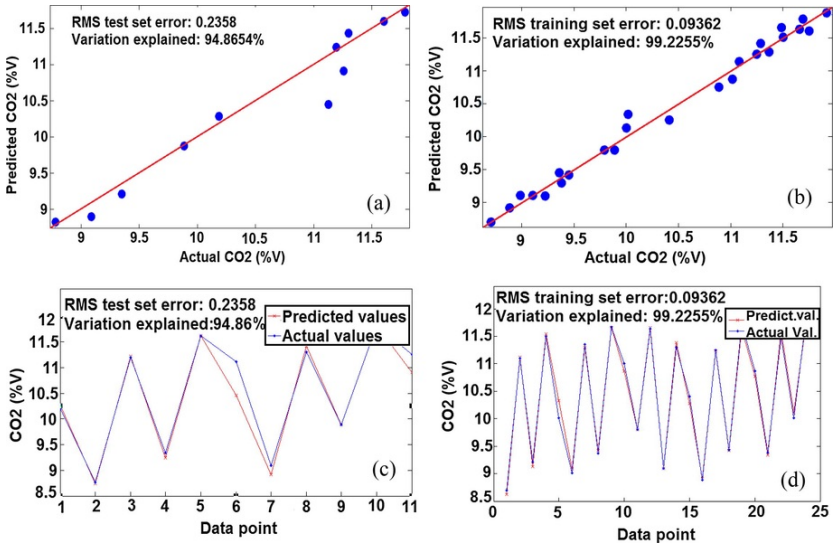

Fig. 21 Measured versus predicted values of CO_2 (a) testing set data, (b) training data set. Experimental results and the GP model prediction of CO_2 for (c) testing set data, (d) training data.

4.2.6 UHC

The following equation was selected as the best model for HC emission:

$$HC = 0.6149\sin(x_1) - 0.2822x_2 - 1.23x_1 + 0.6149\tanh(x_3) - 2073\cos(\tanh(x_1 - 2x_2 + x_3)) + 0.1573 psqroot(p\log(x_2))\cos(x_1) - 0.1573\sin(-x_2 - 9.769)\sin(x_1) - 0.2073x_1\tanh(x_3) + 0.2073x_3\cos(x_1 + x_2)\cos(x_1) + 0.1191 \quad (10)$$

where HC is the HC emission (ppm). Accuracy of the equation is studied by plotting the measured values versus predicted by GP values for training and testing sets (Fig. 22). The values of R^2 and RMSE are 0.9388 and 0.8699 respectively for testing set (Fig. 22a) and 0.9961 & 0.2439 respectively for training set (Fig. 22b). There is a good correlation between the predictions from multi-gene GP and the measured data. A comparison of the error during testing and training by using GP and experimental results has been illustrated in Fig. 22c & d. It was proved that the multi-gene GP model can predict HC with a high variation explained (93.886% for testing and 99.61% for training) and very low root mean square (RMS) error (0.8699 for testing and 0.2439 for training).

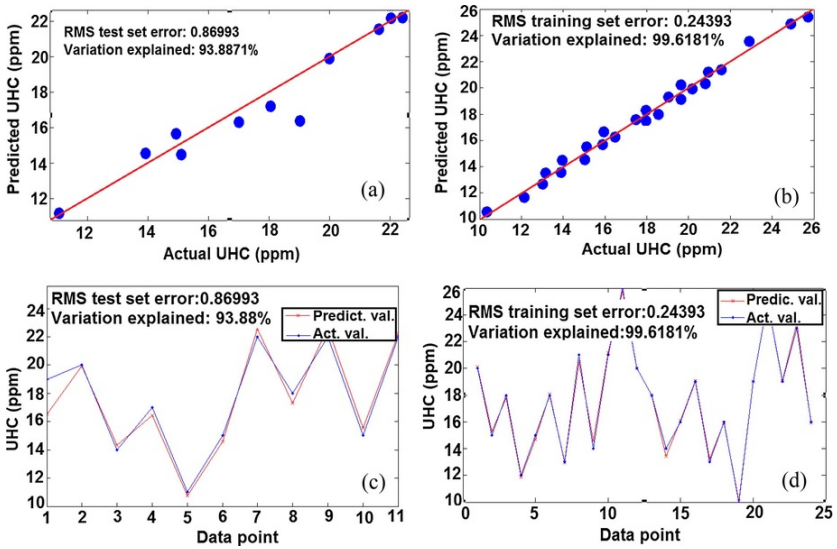

Fig. 22 Measured versus predicted values of UHC emission (a) testing set data, (b) training data set. Experimental results and the GP model prediction of UHC for (c) testing set data, (d) training data.

4.2.7 Nox

The following equation was selected as the best model for NO_x emission:

$$NO_x = 1.184\tanh(\tanh(\tanh(x_1)) - 0.2114) - 0.2048\exp(5.262x_2\tanh(x_3)) + 0.04838\sin(x_2 + \tanh(x_1) - 6.525) + 0.04849\exp(x_2 - 1.0x_1) - 0.2048\tanh(5.262x_2 + \cos(x_1)) + 0.4438 \quad (11)$$

Accuracy of the equation is studied by plotting the measured values versus predicted by GP values for training and testing sets (Fig. 23). The values of R^2 and RMSE are 0.9843 and 23.169 respectively for testing set (Fig. 23a) and 0.9884 & 23.22 respectively for training set (Fig. 23b). There is a good correlation between the predictions from multi-gene GP and the measured data. A comparison of the error during testing and training by using GP and experimental results has been illustrated in Fig. 23c & d. It was proved that the multi-gene GP model can predict NO_x with a high variation explained (98.43% for testing and 98.84% for training) and very low root mean square (RMS) error (23.16 for testing and 23.22 for training).

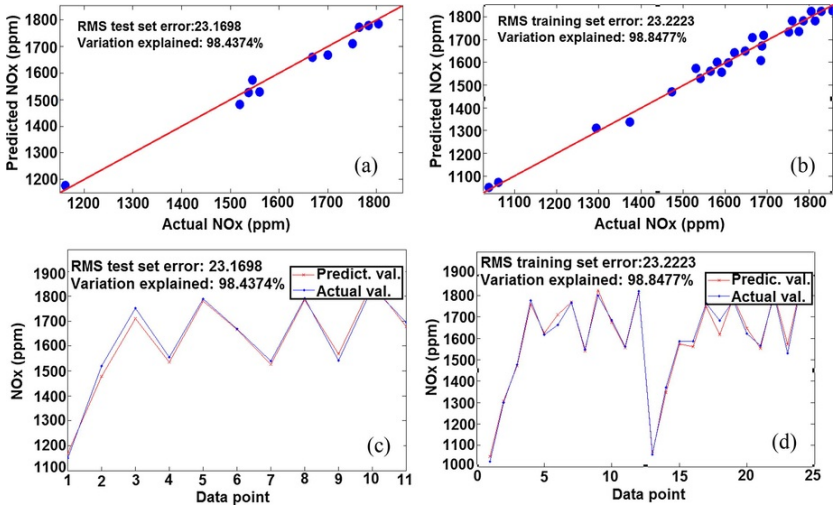

Fig. 23 Measured versus predicted values of NO_x emission (a) testing set data, (b) training data set. Experimental results and the GP model prediction of NO_x for (c) testing set data, (d) training data.

Due to comparison, R^2 and RMSE values for Performance & Emission parameters are listed in Table 7. Experimental Data analysis by the GP revealed that there is a good correlation between the GP predicted results and the experimental data (Table 6). Therefore GP proved to be a useful tool for correlation and simulation of engine parameters.

Table 7 R^2 and RMSE values for Performance & Emission parameters.

	Parameters	Train set		Test set	
		R^2	RMSE	R^2	RMSE
Performance parameters	Power	0.9995	0.0458	0.9995	0.0901
	Torque	0.9993	0.3885	0.9965	0.8886
	BSFC	0.9678	1.15	0.9477	1.55
Emission parameters	CO	0.9922	0.0934	0.9337	0.2678
	CO2	0.9922	0.0936	0.9486	0.2358
	UHC	0.9961	0.2439	0.9388	0.8699
	Nox	0.9884	23.22	0.9843	23.16

5 Conclusions

The present work demonstrates that the use of nano-diesel-biodiesel blended fuel will increase the brake power and torque and decrease the brake specific fuel consumption. It was also found that the CO_2 and NO_x concentrations were increased while the concentration of CO and HC were decreased when nano-biodiesel-diesel blends are used. The multi-gene genetic programming results are very good, R values in this model are very close to one, while root mean square errors (RMSE) were found to be very low. Analysis of the experimental data by the GP revealed that there is a good correlation between the GP predicted results and the experimental data. Therefore GP proved to be a useful tool for correlation and simulation of engine parameters. GP provided an accurate and simple approach in the analysis of this complex, multivariate problem, the analysis of the CI engine performance and emissions.

References

[1] V. Arul Mozhi Selvan, R.B. Anand and M. Udayakumar, Effects of cerium oxide nanoparticle addition in diesel and diesel-biodiesel-ethanol blends on the performance and emission characteristics of a CI engine, *ARPN J Eng Appl Sci* **4** (7), 2009, 1–6.

[2] H. Jung, D.B. Kittelson and M.R. Zachariah, The influence of a cerium additive on ultrafine diesel particulate emissions and kinetic of oxidation, *Combust Flame* **142**, 2005, 276–288.

[3] V. Sanchez Escribano, E. Fernandez Lopez, J.M. Gallardo-Amores, C. del Hoyo Martínez, C. Pistarino, M. Panizza, et al., A study of a ceria-zirconia-supported manganese oxide catalyst for combustion of diesel soot particles, *Combust Flame* **153**, 2008, 97–104.

[4] H. Idriss, Ethanol reactions over the surface of noble metal/cerium oxide catalysts, *Platinum Metals Rev* **48** (3), 2004, 105–115.

[5] B. Park, K. Donaldson, R. Duffin, L. Tran, F. Kelly, I. Mudway, et al., Hazard and risk assessment of a nano-particulate cerium oxide based diesel fuel additive-a case study, *Inhalation Toxicol* **20** (6), 2008, 547–566.

[6] S. Safari Kish, A. Rashidi, H.R. Aghabozorg and L. Moradi, Increasing the octane number of gasoline using functionalized carbon nanotubes, *Appl Surf Sci* **256**, 2010, 3472–3477.

[7] Massie DD. Neural-network fundamentals for scientists and engineers. In: Efficiency, cost, optimization, simulation and environmental impact of energy systems ECOS'01, Istanbul, Turkey; July 4–6, 2001. p. 123–131.

[8] J.H. Holland, Adaptation in Natural and Artificial Systems, 1975, University of Michigan Press; Ann Arbor.

[9] M. Gen and R. Cheng, Genetic Algorithms and Engineering Design, 1997, Wiley; London.

[10] N.M. Kwok, D.K. Liu and G. Fang, Evolutionary computing based mobile robot localization, *Eng Appl Artif Intell* **19** (8), 2006, 857–868.

[11] M. Izadifar and M.Z. Jahromi, Application of genetic algorithm for optimization of vegetable oil hydrogenation process, *Appl Therm Eng* **78**, 2007, 1–8.

[12] T. Laukkanen, T. Tveit, V. Ojalehto, K. Miettinen and C. Fogelholm, Bilevel. Heat exchanger network synthesis with an interactive multi-objective optimization method, *Appl Therm Eng* **48**, 2012, 301–316.

[13] J. Tsai, An evolutionary approach for worst-case tolerance design, *Eng Appl Artif Intell* **25**, 2012, 917–925.

[14] L. Gusel and M. Brezocnik, Application of genetic programming for modelling of material characteristics, *Expert Syst Appl* **38**, 2011, 15014–15019.

[15] U.K. Chakraborty, Static and dynamic modeling of solid oxide fuel cell using genetic programming, *Energy* **34**, 2009, 740–751.

[16] H.H. Chang, Genetic algorithms and non-intrusive energy management system based economic dispatch for cogeneration units, *Energy* **36** (1), 2011, 181–190.

[17] M. Karakus, Function identification for the intrinsic strength and elastic properties of granitic rocks via genetic programming (GP), *Comput Geosci* **37** (9), 2011, 1818–1323.

[18] M. Pala, Genetic programming-based formulation for distortional buckling stress of cold-formed steel members, *J Constr Steel Res* **64**, 2008, 1495–1504.

[19] M. Asadi, M. Eftekhari and M.H. Bagheripour, Evaluating the strength of intact rocks through genetic programming, *Applied Soft Computing* **11**, 2011, 1932–1937.

[20] C. Fonlupt, Solving the ocean color problem using a genetic programming approach, *Applied Soft Computing* **1**, 2001, 63–72.

[21] B. Can and C. Heavey, Comparison of experimental designs for simulation-based symbolic regression of manufacturing systems, *Comput Ind Eng* **61** (3), 2011, 447–462.

[22] H.C. Tsai, Using weighted genetic programming to program squat wall strengths and tune associated formulas, *Eng Appl Artif Intell* **24**, 2011, 526–533.

[23] J.C.M. Pires, M.C.M. Alvim-Ferraz, M.C. Pereira and F.G. Martins, Prediction of tropospheric ozone concentrations: application of a methodology based on the Darwin's Theory of Evolution, *Expert Syst Appl* **38**, 2011, 1903–1908.

[24] A. Baykasoglu, H. Gullu, H. Canak and L. Ozbakir, Prediction of compressive and tensile strength of limestone via genetic programming, *Expert Syst Appl* **35**, 2008, 111–123.

[25] A. Cevik and A.F. Cabalar, Modelling damping ratio and shear modulus of sand-mica mixtures using genetic programming, *Expert Syst Appl* **36** (4), 2009, 7749–7757.

[26] Hinchliffe MP, Willis MJ, Hiden HG, Tham MT, McKay B, Barton G. Modelling Chemical Process Systems Using a Multi-Gene Genetic Programming Algorithm. In: proceedings of the First Annual Conf on Genetic programming (Late Breaking Paper). 1996; pp. 56–65.

[27] H.G. Hiden, Data-Based Modelling using Genetic Programming, PhD Thesis1998, Dept. Chemical and Process Engineering, University of Newcastle; UK.

[28] M.H. Baziar, Y. Jafarian, H. Shahnazari, V. Movahed and M.A. Tutunchian, Prediction of strain energy-based liquefaction resistance of sand–silt mixtures: an evolutionary approach, *Comput Geosci* **37**, 2011, 1883–1893.

[29] H.M. Chen, W.K. Kao and H.C. Tsai, Genetic programming for predicting aseismic abilities of school buildings, *Eng Appl Artif Intell* **25**, 2012, 1103–1113.

[30] M. Kiani, B. Ghobadian, F. Ommi and G. Najafi, Application of genetic programming to predict an SI engine brake power and torque using ethanol-gasoline fuel blends, *Int J Nat Eng Sci* **7** (3), 2013, 7–15.

[31] J.M. Alonso, F. Alvarruiz, J.M. Desantes, L. Hernández, V. Hernández and G. Moltó, Combining neural networks and genetic algorithms to predict and reduce diesel engine emission, *IEEE Trans Evol Comput* **11**, 2007, 46–55.

[32] U. Kesgin, Genetic algorithm and artificial neural network for engine optimization of efficiency and NOX emission, *Fuel* **83**, 2004, 885–895.

[33] K. Atashkari, N. Nariman-Zadeh, M. Gölcü, A. Khalkhali and A. Jamali, Modelling and multi-objective optimization of a variable valve-timing spark-ignition engine using polynomial neural networks and evolutionary algorithms, *Energy Convers Manage* **48**, 2007, 1029–1041.

[34] Z. Yang, L. Wang and S. Li, Investigation into the optimization control technique of hydrogen-fueled engines based on genetic algorithms, *Int J Hydrogen Energy* **33**, 2008, 6780–6791.

[35] Hiroyasu T, Miki M, Kamiura J, Watanabe S, Hiroyasu H. Multi-objective optimization of diesel engine emissions and fuel economy using genetic algorithms and phenomenological model. SAE 2002[paperno:01–2778].

[36] G. Cai, J. Fang, X. Xu and M. Liu, Performance prediction and optimization for liquid rocket engine nozzle, *Aerosp Sci Technol* **11**, 2007, 155–162.

[37] R. Verma and P.A. Lakshminarayanan, A case study on the application of a genetic algorithm for optimization of engine parameters, *Pl Mech Eng D-J Automobile Eng* **220** (4), 2006, 471–479.

[38] X.Y. Tong, G.B. Cai, Y.T. Zheng and J. Fang, Optimization of system parameters for gas generator engines, *Acta Astronaut* **59**, 2006, 246–252.

[39] J.R. Koza, Genetic programming: On The Programming of Computers by Means of Naturals Election, 1992, MIT Press; Cambridge, MA.

[40] J.J. Wang, Y.Y. Jing and C.F. Zhang, Optimization of capacity and operation for CCHP system by genetic algorithm, *Appl Energy* **87**, 2010, 1325–1335.

[41] B. Saerens, J. Vandersteen, T. Persoons, J. Swevers, M. Diehl and E. Bulk, Minimization of the fuel consumption of a gasoline engine using dynamic optimization, *Appl Energy* **86**, 2009, 1582–1588.

[42] I. Al-Hinti, M. Samhouri, A. Al-Ghandoor and A. Sakhrieh, The effect of boost pressure on the performance characteristics of a diesel engine: a neuro-fuzzy approach, *Appl Energy* **86**, 2009, 113–121.

[43] C. Evans, P.J. Fleming, D.C. Hill, J.P. Norton, I. Pratt and D. Rees, Application of system identification techniques to aircraft gas turbine engines, *Control Eng Pract* **9**, 2001, 135–148.

[44] A.E. Ruano, P.J. Fleming, C. Teixeira, K. Rodríguez-Vázquez and C.M. Fonseca, Nonlinear identification of aircraft gas-turbine dynamics, *Neuro Computing* **55**, 2003, 551–579.

[45] V. Arkov, C. Evans, P.J. Fleming, D.C. Hill, J.P. Norton and I. Pratt, System identification strategies applied to aircraft gas turbine engines, *Annu Rev Control* **24**, 2000, 67–81.

[46] G.J. Gray, D.J. Murray-Smith, Y. Li, K.C. Sharman and T. Weinbrenner, Nonlinear model structure identification using genetic programming, *Control Eng Pract* **6**, 1998, 1341–1352.

[47] S.A. Kalogirou, Artificial intelligence for the modeling and control of combustion processes: a review, *Prog Energy Combust* **29**, 2003, 515–566.

[48] N.K. Togun and S. Baysec, Prediction of torque and specific fuel consumption of a gasoline engine by using artificial neural networks, *Appl Energy* **87**, 2010, 349–355.

[49] N. Togun and S. Baysec, Genetic programming approach to predict torque and brake specific fuel consumption of a gasoline engine, *Appl Energy* **87**, 2010, 3401–3408.

[50] P. Chand, V.R. Chintareddy, J.G. Verkade and D. Grewell, Enhancing biodiesel production from soybean oil using ultrasonics, *Energy Fuels* **24**, 2010, 2010–2015.

[51] E. Fayyazi, B. Ghobadian, G. Najafi and B. Hosseinzadeh, Genetic algorithm approach to optimize biodiesel production by ultrasonic system, *Chem Prod Process Model* 2013, 1–12.

[52] A.M. Rashidi, M.M. Akbarnejad, A.A. Khodadadi, Y. Mortazavi and A. Ahmadpour, Single wall carbon nano tubes synthesized using organic additives to Co–Mo catalysts supported on nano porous MgO, *Nanotechnology* **18**, 2007, 315605.

[53] S. SafariKish, A.M. Rashidi, H.R. Aghabozorg and L. Moradi, Increasing the octane number of gasoline using functionalized carbon nano tubes, *Appl Surf Sci* **256**, 2010, 3472–3477.

[54] H. Bayraktar, Experimental and theoretical investigation of using gasoline–ethanol blends in spark-ignition engines, *Renew Energy* **30**, 2005, 1733–1747.

[55] M.B. Celik, Experimental determination of suitable ethanol–gasoline blend rate at high compression ratio for gasoline engine, *Appl Therm Eng* **28**, 2008, 396–404.

[56] M. Al-Hasan, Effect of ethanol-unleaded gasoline blends on engine performance and exhaust emissions, *Energy Conv Manage* **44**, 2003, 1547–1561.

[57] W.D. Hsieh, R.H. Chen, T.L. Wu and T.H. Lin, Engine performance and pollutant emission of an SI engine using ethanol–gasoline blended fuels, *Atmos Environ* **36**, 2002, 403–410.

[58] A.K. Agarwal, Biofuels (alcohols and biodiesel) applications as fuels for internal combustion engines, *Prog Energy Combust Sci* **33**, 2007, 233–271.

[59] Z. Mouloungui, G. Vaitilingom, J.C. Berge and P.S. Caro, Interest of combining an additive with diesel ethanol blends for use in diesel engines, *Fuel* **80** (4), 2001, 565–574.

[60] C.W. Wu, R.H. Chen, J.Y. Pu and T.H. Lin, The influence of air–fuel ratio on engine performance and pollutant emission of an SI engine using ethanol–gasoline- blended fuels, *Atmos Environ* **38**, 2004, 7093–7100.

[61] J.R. Koza, Genetic Programming: On the Programming of Computers by Means of Natural Selection, 1992, MIT Press; Cambridge.

[62] B. Can and C. Heavey, A comparison of genetic programming and artificial neural networks in meta modeling of discrete-event simulation models, *Comput Oper Res* **39**, 2012, 424–436.

[63] D.P. Searson, GPTIPS: Genetic Programming & Symbolic Regression for MATLAB, Available at:http://gptips.sourceforge.net, 2009.

[64] Searson DP. 2009b. GPTIPS: Genetic Programming & Symbolic Regression for MATLAB, User Guide.

[65] D.C. Rakopoulos, C.D. Rakopoulos and E.G. Giakoumis, Impact of properties of vegetable oil, bio-diesel, ethanol and n-butanol on the combustion and emissions of turbocharged HDDI diesel engine operating under steady and transient conditions,

Fuel **156**, 2015, 1–19.

[66] D.C. Rakopoulos, C.D. Rakopoulos and D.C. Kyritsis, Butanol or DEE blends with either straight vegetable oil or biodiesel excluding fossil fuel: comparative effects on diesel engine combustion attributes, cyclic variability and regulated emissions trade-off, *Energy* **115**, 2016, 314–325.

[67] Harish Venu and Venkataramanan Madhavan, Effect of Al_2O_3 nanoparticles in biodiesel-diesel-ethanol blends at various injection strategies: performance, combustion and emission characteristics, *Fuel* **186** (15), 2016, 176–189.

[68] Khadijeh Heydari-Maleney, Ahmad Taghizadeh-Alisaraei, Barat Ghobadian and Ahmad Abbaszadeh-Mayvan, Analyzing and evaluation of carbon nanotubes additives to diesohol-B2 fuels on performance and emission of diesel engines, *Fuel* **196** (15), 2017, 110–123.

[69] V. Arul Mozhi Selvan, R.B. Anand and M. Udayakumar, Effect of cerium oxide nanoparticles and carbon nanotubes as fuel-borne additives in diesterol blends on the performance, combustion and emission characteristics of a variable compression ratio engine, *Fuel* **130** (15), 2014, 160–167.

[70] Mehrdad Mirzajanzadeh, Meisam Tabatabaei, Mehdi Ardjmand, Alimorad Rashidi, Barat Ghobadian, Mohammad Barkhi, et al., A novel soluble nano-catalysts in diesel–biodiesel fuel blends to improve diesel engines performance and reduce exhaust emissions, *Fuel* **139**, 2015, 374–382.

[71] B. Rajesh Kumar and S. Saravanan, Partially premixed low temperature combustion using dimethyl carbonate (DMC) in a DI diesel engine for favorable smoke/NOx emissions, *Fuel* **180**, 2016, 396–406.

[72] Pravesh Chandra Shukla, Tarun Gupta, Nitin Kumar Labhsetwar and Avinash Kumar Agarwal, Trace metals and ions in particulates emitted by biodiesel fuelled engine, *Fuel* **188**, 2017, 603–609.

[73] Sergio Manzetti and Otto Andersen, A molecular dynamics study of nanoparticle-formation from bioethanol-gasoline blend emissions, *Fuel* **183**, 2016, 55–63.

[74] Ajin C. Sajeevan and V. Sajith, Synthesis of stable cerium zirconium oxide nanoparticle – diesel suspension and investigation of its effects on diesel properties and smoke, *Fuel* **183**, 2016, 155–163.

[75] Lijian Leng, Xingzhong Yuan, Guangming Zeng, Xiaohong Chen, Hou Wang, Hui Li, et al., Rhamnolipid based glycerol-in-diesel microemulsion fuel: formation and characterization, *Fuel* **147**, 2015, 76–81.

[76] Soner Gumus, Hakan Ozcan, Mustafa Ozbey and Bahattin Topaloglu, Aluminum oxide and copper oxide nanodiesel fuel properties and usage in a compression ignition engine, *Fuel* **163**, 2016, 80–87.

[77] Ahmad Fayyazbakhsh and Vahid Pirouzfar, Investigating the influence of additives-fuel on diesel engine performance and emissions: analytical modeling and experimental validation, *Fuel* **171** (1), 2016, 167–177.

[78] Soner Gumus, Hakan Ozcan, Mustafa Ozbey and Bahattin Topaloglu, Aluminum oxide and copper oxide nanodiesel fuel properties and usage in a compression ignition engine, *Fuel* **163** (1), 2016, 80–87.

[79] G. Najafi, B. Ghobadian, R. Mamat, T. Yusaf and W.H. Azmi, Solar energy in Iran: current state and outlook, *Renew Sustain Energy Rev* **49**, 2015, 931–942.

[80] A. Abbaszadeh, B. Ghobadian, G. Najafi and T. Yusaf, An experimental investigation of the effective parameters on wet washing of biodiesel purification, *Int J Automot Mech Eng* **9** (1), 2014, 1525–1537.

[81] G. Najafi and B. Ghobadian, LLK1694-wind energy resources and development in Iran, *Renew Sustain Energy Rev* **15** (6), 2011, 2719–2728.

[82] G. Najafi, B. Ghobadian, A. Moosavian, T. Yusaf, R. Mamat, M. Kettner, et al., SVM and ANFIS for prediction of performance and exhaust emissions of a SI engine with gasoline-ethanol blended fuels, *Appl Therm Eng* **95**, 2016, 186–203.

[83] E. Fayyazi, B. Ghobadian, G. Najafi, B. Hosseinzadeh, R. Mamat and J. Hosseinzadeh, An ultrasound-assisted system for the optimization of biodiesel production from chicken fat oil using a genetic algorithm and response surface methodology, *Ultraso*
Sonochem **26**, 2015, 312–320.

[84] P. Nematizade, B. Ghobadian and G. Najafi, Investigation of fossil fuel and liquid biofuel blend properties using artificial neural network, *Int J Automot Mech Eng* **5** (1), 2012, 639–647.

Highlights

- Using nano-diesel-biodiesel increased the brake power, torque and decrease bsfc of CI engine.
- The CO_2 and NO_x increased while the concentration of CO and HC were decreased with nano-biodiesel-diesel blends.

- Good correlation was observed between genetic programming predicted results and experimental data.
- GP proved to be a useful tool for correlation and simulation of engine parameters.
- GP provided an accurate and simple approach in the analysis of the CI engine performance and emissions.